PHYSICAL REVIEW B VOLUME 39, NUMBER 6 15 FEBRUARY 1989-II

Electronic structure of Ge/Si monolayer strained-layer superlattices

T. P. Pearsall, J. Bevk, J. C. Bean, J. Bonar, and J. P. Mannaerts
AT&T Bell Laboratories, Murray Hill, New Jersey 07974-2070

A. Ourmazd
AT&T Bell Laboratories, Holmdel, New Jersey 07733-1988
(Received 20 May 1988; revised manuscript received 3 November 1988)

We report the results of a study of Ge/Si strained-layer superlattices grown on (001) Si substrates. These results allow us to study the transition between superlattice and bulk states. We have examined samples whose superlattice period lies between 3 and 15 Å, similar to the lattice parameter of the crystalline unit cell. All of the samples in this study are ordered superlattices with an average composition of $Ge_{0.5}Si_{0.5}$. Intentional ordering on a monolayer scale was achieved by molecular-beam epitaxy. The optical energy-level spectra of these structures at critical points in the Brillouin zone were measured by Schottky-barrier electroreflectance in the energy range 0.6 to 4 eV. Some features of these spectra can be attributed to the creation of new band-to-band optical transitions that are induced by the artificial periodicity imposed on the sample during growth. These new energy levels are derived from bulk Si and Ge energy levels modified by heterojunction offset, strain, and the lower symmetry of the new unit cell. Several of the new optical transitions observed between 0.6 and 1.5 eV are normally forbidden or weakly allowed. The observation of relatively strong transition amplitudes in electroreflectance suggests that electric field effects and deviations from an ideal diamond-lattice structure may play an important role in the enchancement of transition probabilities in superlattice structures.

I. INTRODUCTION

Ge/Si strained-layer epitaxy consists of the commensurate, lattice-mismatched growth of heterostructures of Ge, Si, and Ge_xSi_{1-x} alloys on a single-crystal (usually Si) substrate. The thickness of the lattice-mismatched layers must be kept under a critical limit to minimize the nucleation of misfit dislocations, and to promote high-quality epitaxy.[1]

Tremendous strides have been made in the control of defects, planarity, and layer thickness. Such advances have made possible recent experiments that demonstrate the capability to achieve significant modifications in the electronic energy-level spectrum of the strained-layer heterostructures.[2–4] These modifications are achieved by exploiting the effects of the extraordinary level of strain frozen into the heterostructure during growth. The strain approaches 4% in samples of pure Ge grown of Si.[5] Equally important are modifications introduced by alloying Ge with Si and quantum size effects. In all cases, these perturbations change the band structure by distortion of the well-known Si or Ge band structures. The magnitudes of the changes can be quite large, shifting some levels by 500 meV or more.[4] Modifications in the bulk band structure provoked by strain, alloying, and quantum size effects have been extensively studied in many semiconductors, and their effects appear to be well understood in most cases in terms of bulk deformation potentials, bulk energy levels, and simple models of one-dimensional carrier confinement. This situation obtains in Ge/Si strained-layer structures where it has been shown that good agreement between energies calculated using the strain-dependent Hamiltonian and experimental measurement obtains even for strains approaching the elastic limit.[4–7]

In our experiments, the concept of strained-layer epitaxy has been carried one step further. We have studied the properties of a series of heterostructures in which the typical layer thickness is comparable to or smaller than the fundamental lattice parameter. One of the principal goals of this work is to use such structures to create a new unit-cell symmetry for a structure containing tetrahedrally bonded Si and Ge. To date, we have examined structures grown on (001) Si substrates. The unit cell of Si along this axis is composed of four atomic monolayers with a total thickness of 5.43 Å. Using molecular-beam epitaxy, we have created planar, layered heterostructures consisting nominally of alternating atomic monolayers of Ge and Si (1:1), alternating two atomic layers of Ge and Si (2:2), alternating four atomic layers of Ge and Si, and alternating six atomic layers of Ge and Si. All of these structures have nearly the same average composition, *to wit*: $Ge_{0.5}Si_{0.5}$. Our initial results demonstrated that the (4:4) structure has an electronic energy spectrum that is qualitatively different from that of the 50%-50% Ge-Si alloy.[8] In particular, new optical transitions have been resolved at energies that cannot be explained by some simple combination derived from those seen in Ge or Si. One of these transitions occurs at an energy lower than any direct transition in either bulk Ge or Si. This result has promoted speculation that particular synthetic Brillouin-zone structures of Ge and Si may be direct, or quasi-direct-gap semiconductors.[9] So far, our experimental results have not yet identified such a case. People and Jackson have pointed out that the lowest-lying states in the conduction band

 ©1989 The American Physical Society

are derived from the ⟨100⟩ valleys of Si.[10] This picture is further supported by detailed calculations of the electronic band structure.[9,11–13] These calculations have confirmed that new transitions with some direct character are created by superlattice and strain-induced mixing of zone-edge and zone-center states. All of these calculations are in relatively good agreement concerning the energies of these new transitions. In addition, these calculated energies correspond to those seen in experiment. However, the calculated matrix elements for these new transitions are quite small for models based on ideal, infinitely extended superlattices.[9,11–13] In some cases theoretical calculation of the transition matrix element suggests that the transition amplitude should be several orders of magnitude less than what is observed in experiment. On the other hand, other calculations that take account of the deviations from an ideal superlattice result in optical transition matrix elements that are in somewhat closer coincidence with experimental results.[10,14,15]

The use of single-element heterostructures involving pure Ge and pure Si, as opposed to compound or alloy semiconductors, makes it possible to define experimentally the boundary between adjacent heterolayers with an accuracy approaching one or two atomic monolayers. The total thickness of the entire superlattice structure is ~ 50 Å. This is nearly small enough for the precise structure on which experimental data are taken to be treatable by a microscopic band-structure calculation. However, such a calculation has not yet been undertaken, and so far all theoretical calculations treat the superlattice structures as infinite extended crystals by invoking periodic boundary conditions.

II. EXPERIMENTAL METHODS

A. Sample preparation

The wafer structure, shown in Fig. 1, was formed by the sequential deposition of 1000 Å of Si buffer layer, followed by the Ge/Si superlattice region, and finally by a 100-Å cap layer. These layers were unintentionally doped and deposited on a conducting (001) Si substrate as described in earlier work.[16,17]

In order to investigate directly the structure of the deposited layers, thin foils were prepared by standard ion-milling techniques to allow the examination of the samples in cross section, with the electron beam parallel to a ⟨110⟩ normal to the growth direction. Lattice images were obtained at a 1.6-Å point-to-point resolution. Under these conditions the interference pattern resulting from the periodic array of pairs of atom columns appears as a black or white blob. The direct observation of monolayer-scale layers is complicated by the presence of interfacial steps that tend to smear out the layers and by the presence of substantial strain. Only Ge or Si layers with thicknesses equal to or greater than four monolayers can be observed clearly by lattice imaging, although some evidence for the presence of layering in the (2:2) Ge/Si samples was also observed.

The samples used for electroreflectance measurement were cut from the wafer following growth. A typical sample area for electroreflectance measurements was 3×6 mm^2. Prior to contact deposition, samples were degreased in boiling acetone followed by rinses in acetone and methanol, and an air dry in a low-particle (class 100) environment. The contacts were electron-beam evaporated. The Schottky barrier was formed on the Si cap layer by an evaporation of a 50-Å, semitransparent Ni film. On a small part of this film, a 2000-Å gold contact stripe was also deposited to facilitate electrical contact during measurement. The back contact was a broad-area deposition of 200 Å Ti followed by 2000 Å Au. The resulting Schottky barriers were of sufficient quality to apply modulation voltages of at least ± 2 V for most samples.

The spectral range of our measurements includes the near ultraviolet where the combination of high photon energy ($\hbar\omega \sim 4$ eV) and high electric field ($E \sim 10^5$ V/cm) could promote Ni migration from the Schottky barrier into the depletion region of the Schottky barrier. Secondary ion-mass spectroscopy on some samples showed negligible Ni presence 500 Å below the sample surface. Therefore, the 1000-Å Si cap layer is sufficiently thick to exclude Ni from diffusion into the superlattice.

Electric field modulation of the reflectance is achieved by biasing the Schottky barrier. Both ac and dc bias was used in order to achieve the maximum amplitude variation. The modulation voltage ranged between 2.0 and 4.0

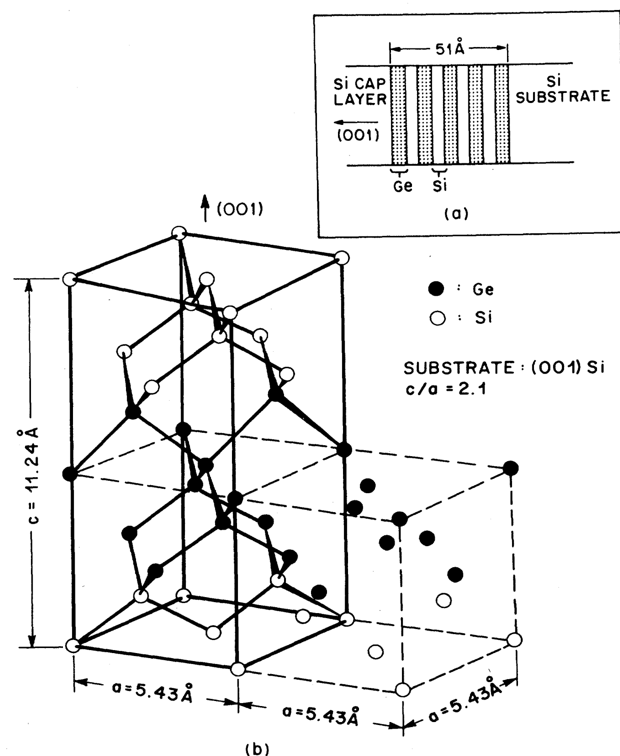

FIG. 1. Diagram of a (4:4) Si/Ge superlattice, one of the strained-layer structures studied in this work. Growth on a relatively thick Si substrate means that subsequent Si epitaxial layers are strain free, so that all the mismatch strain is imposed on the Ge layers.

V peak-to-peak ac. The magnitude of the applied field was limited by both the quality of the Schottky barrier and the voltage source used, but care was taken to measure all samples under similar modulation conditions.

The Ni Schottky barrier permits the sample to be reverse biased to an electric field of about 2.5×10^4 V/cm. A more precise determination of the electric field strength was not made because the carrier-concentration profile in the superlattice region is nonuniform, and, in general, difficult to determine precisely. Since the field is applied from the epitaxial side of the wafer, it must deplete only 1000 Å to reach the superlattice region. As the field on the sample is modulated, the edge of the depletion region will sweep though the superlattice.

B. Electroreflectance spectroscopy

Electroreflectance spectra were taken at room temperature over the energy range 0.6–4.0 eV. A 100-W tungsten lamp was used as the light source in the ir, and a 150-W xenon arc lamp was used in the uv, visible, and ir. The wavelength was scanned using a McPherson monochromator with an effective aperture of $f/6.4$. The wavelength resolution of the experiment, dependent on the grating and slit width, is about 12 Å. This is much finer than the linewidth of the features discussed in our results.

Borosilicate glass optics were used. The reflected light was detected using an S-20 photomultiplier tube in the uv and visible, from 2 to 4 eV. The tube has a borosilicate glass envelope which does not transmit above 4 eV and so acts as a filter. A lead sulfide photoconductive cell, cooled to 220 K, was used to cover the red and infrared from 0.6 to 2 eV. Appropriate filters were used to eliminate higher-than-first-order transmission through the grating.

The spectra were taken by collecting the reflected light, which consists of a small ac component (typically 10^{-3}–10^{-5} times smaller) superimposed on a large dc component. The total reflected light R is measured and digitized by a dc voltmeter. The modulated component of the signal, ΔR, is separated from the total reflected light signal by the lock-in amplifier. The values of R and ΔR are recorded digitally and their ratio is calculated. The entire experiment is under the control of an AT&T PC6300 computer. Since the monochromator is stepped rather than continuously scanned, we take multiple readings at each wavelength, permitting signal averaging. In addition, the analog averaging feature of the lock-in amplifier is used to improve the signal-to-noise ratio. The resolution of the measurement is dependent on the dynamic range of the detectors and the inherent noise in the experiment. In practice, we can measure $\Delta R/R$ in the low-10^{-7} range. These techniques have extended the sensitivity of electroreflectance spectroscopy by several orders of magnitude.

The advantage of measuring the ratio of modulated reflected light to total reflected light is that the ratio $\Delta R/R$ is, in principle, independent of the light intensity, grating, light source, or absorption by optical components. The rationalization of data, however, will not correct for nonlinear distortions introduced by the experiment. Recent advances reported by Shen *et al.*, could be used to eliminate this difficulty.[18] In practice, this procedure makes it possible to compare directly data from different wavelength regions, taken with different gratings, light sources, detectors, and even different samples.

Electroreflectance measurements on bulk Ge were first taken as a means of verifying both data acquisition and analysis. Ge has optical transitions at critical points near 0.8, 2.1, and 3.0 eV, covering the energy range of interest in our experiments. The electroreflectance spectrum at 295 K is shown in Fig. 2. These sets of transitions corresponding to E_0 at Γ, E_1 along Λ, and E_0' also at Γ can be identified easily. The electroreflectance spectrum was analyzed by fitting a Lorentzian line-shape function to the data. Results are shown in Table I and the transition energies can be seen to be in excellent agreement with accepted values for these transitions.

III. EXPERIMENTAL MEASUREMENT OF CRITICAL-POINT ENERGIES

A. Analysis of data

Measured values for the electroreflectance ($\Delta R/R_0$) and photon energy ($\hbar\omega$) were recorded at intervals of 10 Å for all samples. Recordings at a finer resolution of 2-Å steps were made for some regions of interest. The data, stored directly on magnetic disk, were analyzed by using a nonlinear convergence routine to fit a line-shape function in order to determine amplitude, transition energy, and linewidth for all the features of the spectrum.

Aspnes has shown that the line shape of the

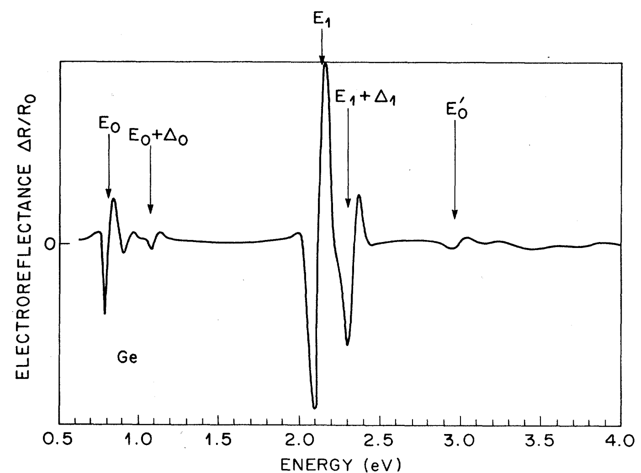

FIG. 2. Electroreflectance spectrum of elemental Ge in the energy range 0.6–4.0 eV. In this range, the E_0, $E_0+\Delta_0$, E_0', and $E_0'+\Delta_0$ transitions at Γ are resolved. The dominant features in the spectrum are the E_1 and $E_1+\Delta_1$ transitions near 2.1 eV.

TABLE I. Measured optical transition energies for Ge.

Peak no.	Energy (eV)	Linewidth (eV)	Origin	Reported values (eV)
1	2.98	0.09	E_0'	2.95[a]
2	2.302	0.086	$E_1+\Delta_1$	2.33[b]
3	2.121	0.063	E_1	2.13[b]
4	1.090	0.041	$E_0+\Delta_0$	1.087[c]
5	0.800	0.036	E_0	0.805[c]

[a]A. K. Ghosh, Phys. Rev. **165**, 888 (1968).
[b]M. Cardona *et al.*, Phys. Rev. **154**, 696 (1967).
[c]B. O. Seraphin *et al.*, J. Appl. Phys. **36**, 2242 (1965).

electroreflectance spectrum of bulk materials is proportional to the third derivative of the dielectric function.[19] The dielectric function near a critical point where an optical transition (that is, $\Delta\mathbf{k}=\mathbf{0}$) can take place may be expressed in terms of the transition energy E_g and the linewidth Γ. In the case of electroreflectance of bulk materials, the actual transition energy is modulated by free carriers that are accelerated by the electric field. This acceleration contributes two out of the three derivatives that are characteristic of the line-shape function. If the carriers are not accelerated by the modulating field because they are confined, or because they are bound in a neutral charge complex such as an exciton, then the electroreflectance spectrum will display only a first-derivative line shape.[20] The electronic excitation spectra of quantum wells and superlattices are dominated by confinement and excitonic effects, and the present study of Ge/Si superlattices presents no exception to these features.

In a typical line-shape analysis, several neighboring transitions are fitted simultaneously. Thus, in the case of Ge, the E_0 and $E_0+\Delta_0$ transitions are fitted to a line-shape function containing two peaks. A third-derivative functional form is used for this analysis because the sample is bulk Ge. For most of the other spectra in this paper, the data range is chosen to include three transitions so that the parameters of every transition are determined relative to those of its neighbors in energy.

The question of the functional form of the transition line shape in electroreflectance has been the subject of recent studies by Shanabrook *et al.*[20] and Zheng *et al.*,[21] with specific reference to the optical properties of quantum-well structures. While the electroreflectance spectra of bulk semiconductors consist often of a few distinct lines, the spectra of quantum-well structures are invariably more complex, with transitions overlapping or nearly overlapping in energy. This situation will distort the observed appearance of the spectrum from the near-classic form seen in Fig. 2.

In these experiments we are interested primarily in determining the energies of optical transitions in Ge/Si superlattice structures. This is the first step in comparing experimentally measured energy levels with band-structure calculations. In the analysis reported here, we have used a Lorentzian line-shape function

$$\frac{\Delta R}{R_0}=\mathrm{Re}[A\Gamma^{-n}e^{i\Phi}(E-E_g-i\Gamma)^{-n}] . \quad (1a)$$

Equation (1a) is fitted to the data by varying the transition amplitude A, the linewidth Γ, the phase Φ, and the transition energy E_g. The transition amplitude is proportional to the square of the standard matrix element for optical transitions. This feature implies that electroreflectance is highly selective in measuring direct optical transitions in homogeneous materials.

The use of Eq. (1a) implies that the measured levels are homogeneously broadened. If variations in superlattice thickness or interface flatness were a major concern, a Gaussian line-shape function would be more appropriate. Our data may be fitted equally well by a Gaussian or Lorentzian line-shape function. Because of experimental conditions related to the nanostructure of the sample, and the temperature, both of which contribute to the relatively broad features seen in our measurements, it does not appear possible to distinguish between these two line-shape functions based on our data. Most important of all, the transition energy is not significantly affected (less than 0.1 eV) by this choice of line-shape function for our data.

The parameter n in Eq. (1a) is related to the nature of the critical point associated with the transition:

$$\begin{aligned} &n=2, \quad \text{exciton or confined} \\ &n=\tfrac{5}{2}, \quad \text{3D, band-to-band} \\ &n=3, \quad \text{2D, band-to-band} \\ &n=\tfrac{7}{2}, \quad \text{1D, band-to-band} . \end{aligned} \quad (1b)$$

(1D, 2D, and 3D denotes one-dimensional, etc.). The value used in line-shape fitting may vary from one energy region of a spectrum to another. For example, the silicon complex near 3.4 eV has its origin in the Si bulk buffer layers and is fitted using $n=\frac{5}{2}$. The Ge/Si superlattices have a basic type-II nature. The valence-band states are confined strongly by the Si buffer layers on each side. However, all the conduction-band states in the superlattice lie higher in energy then the silicon buffer-layer conduction-band edge. Despite this type-II nature of the band gap, we have shown that the energy levels of direct transitions in Ge/Si quantum wells measured in electroreflectance are determined by quantum confinement of carriers by states of the same symmetry in both the quantum-well and barrier region. Thus, the E_0 transition near 2.5 eV is confined by a 2-eV E_0 barrier in the Si buffer layer, even though the indirect conduction-band edge in the Si barrier lies below the E_0 edge.[4] Using this result, it seems appropriate to use $n=2$ corresponding to an excitonic or confined transition when fitting this structure. On the other hand, measured transitions near the indirect edge involve holes that are confined and electrons that are not confined by the Si barrier regions. The line shape of these transitions will be affected by both the first-derivative nature of the holes and the third-derivative nature of the electrons. The experimental results will be best fitted by a line-shape function using an $n_{\mathrm{effective}}$ between 2 and $\frac{7}{2}$, but the physical

significance of n is diminished. However, as in the case of the choice between Gaussian and Lorentzian fitting functions, we have verified that the transition energy changes by less than 0.1 eV as n is varied from 2 to $\frac{7}{2}$. Only the deduced linewidth and amplitude are significantly affected.

The issue of the physical validity of line-shape functions and parameters is important and an area where a great deal of research needs to be done. While our fitting procedure will yield the correct transition energies, it could also provide additional information on interfacial flatness, optical matrix elements, and critical-point dimensionality. Improved knowledge in these three areas would represent a significant advance in the understanding of the physics and microstructure of these superlattice structures.

The proximity in energy of several transitions leads to possible interferences and distortions in the measured spectra. While it is easy to see how amplitude effects, such as superposition of transition peaks, can occur, there is a more subtle effect related to the role that the real and imaginary parts of the dielectric function can play. As discussed by Zheng *et al.*[21] the dielectric function responsible for the electroreflectance spectrum may be dispersive, as in Fig. 2, or dissipative in nature. In the fitting function, the phase is used to account for this feature, and the relative phase difference between two adjacent peaks is an essential component of the fitting procedure. It is important to realize, however, that a purely dissipative dielectric function will result in a strong absorption only if the matrix element is large also.

In strongly inhomogeneous materials, such as the superlattice structures under investigation in this paper, the electric field has a symmetry-breaking effect that enhances the transition matrix element for symmetry-forbidden direct optical transitions. Thus, while the conventional interpretation of electroreflectance has been that it measures only allowed direct optical transitions, the situation can be different in the case of electroreflectance spectroscopy of quantum wells.[22] The presence of a large electric field (10^3–10^5 V/cm) will couple the $n=1$ quantum-well state in the valence band to an $n=2$ state in the conduction band, permitting the observation of a direct optical transition that would be forbidden at zero field.[23] In the experiments of Meynadier *et al.*,[24] it was observed that the strongest feature in the photoluminescence spectrum of type-II AlAs/GaAs superlattices comes from a normally "symmetry-forbidden" transition. In this case, the electric field is used to "tune" the fine details of the lowest-energy bands as well as enhancing transitions to zone-edge (X-like) states.

Finally, we wish to point out that interference effects of a much more common nature can occur in electroreflectance when structures in the sample form a Fabry-Perot étalon. These interference effects can be seen when the wavelength of light is similar to the distance separating the two planes responsible for the interference. This distance λ_0 can be calculated from Eq. (2) by recording the interference period $\Delta\lambda$:

$$\lambda_0=\frac{2\,\Delta M}{\Delta\lambda}\frac{\lambda^2}{[\lambda(\delta n_0/\delta\lambda)-n_0]}\ , \tag{2}$$

where ΔM is the difference in oscillation index. The quantity in the square brackets in Eq. (2) can usually be approximated by an effective index of refraction n^*.

The shortest wavelength of light used in our experiments is 3000 Å, which is reduced by the index of refraction to about 1000 Å in Si or Ge. The superlattice structures reported in this work have a total thickness of about 50 Å, and so we cannot measure interference effects from the superlattices over the spectral range covered in the measurements. Fabry-Perot oscillations are seen in some samples. In Fig. 3 we show such oscillations that obscure most of the region of interest. Using Eq. (2), it is deduced that the fundamental spacing is about 400 μm, or the wafer thickness. These oscillations are seen because of electric field modulation of the carrier distribution at the front and back faces of the sample. While such interference effects may occur, they have a recognizable signature, and they are related to features in the sample geometry much larger than the superlattice plane separation used in our samples.

B. Basic features of the energy spectrum of strained Ge/Si quantum wells

Because Si and Ge are closely related materials, Ge-Si alloys have an electronic structure that can be approximated by an appropriately weighted linear average of the band structures of Ge and Si.[25] In Fig. 4 we show a schematic band structure derived using the virtual-crystal approximation for a strained $Ge_{0.5}Si_{0.5}$ alloy along major symmetry directions in the Brillouin zone. Superimposed on this diagram are the principal direct optical transitions that contribute to the electroreflectance spectrum: E_1 and $E_1+\Delta_1$, which result from a critical point along the $\langle 111 \rangle$ directions, and E_0 and $E_0+\Delta_0$, which result from critical points at the zone center. In our experience

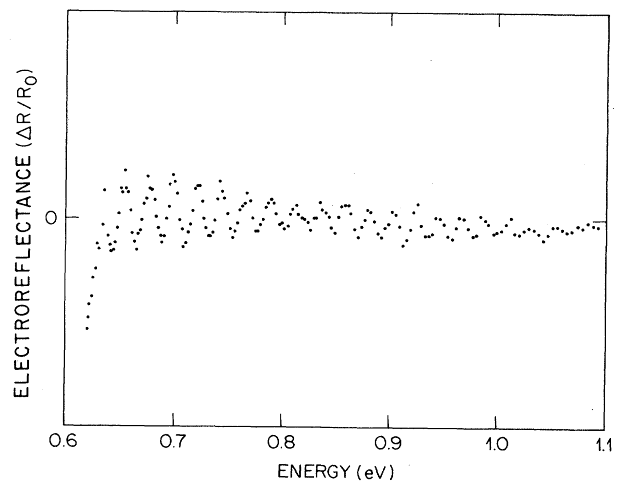

FIG. 3. Electroreflectance spectra can be distorted by the presence of interference oscillations. The wavelength of light used restricts these effects to structures whose physical separation is much greater than the superlattice thickness. In this case, oscillations arise because of interference effects associated with the front and back surfaces of the sample.

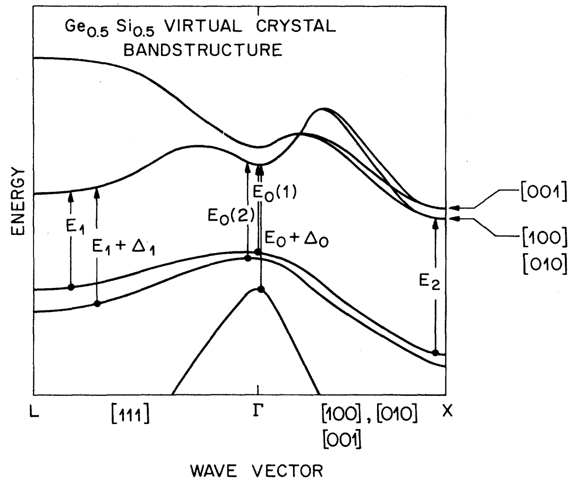

FIG. 4. Schematic electronic band structure of a $Ge_{0.5}Si_{0.5}$ alloy under uniaxial tension along the [001] axis. The energy-momentum diagram is shown for the two nonequivalent ⟨100⟩ directions. Because $Ge_{0.5}Si_{0.5}$ is an indirect-band-gap alloy with conduction-band minima along the ⟨100⟩ directions, uniaxial strain, regardless of sign, along a ⟨100⟩ direction, will *always* lower the band gap. The lower-lying minima will be directed along the axis or (axes) in compression.

with Ge-Si alloys, the E_1 transition is the most important feature in the electroreflectance spectrum.

Under the effects of uniaxial strain that results from the commensurate epitaxial growth of $Ge_{0.5}Si_{0.5}$ on a Si substrate, some of these levels are split. If the substrate surface is perpendicular to the [001] direction, then this axis will be under tensile strain, while the two other ⟨100⟩ directions, which define the plane of epitaxial growth, will be under compressive strain. This situation is directly reflected in the electronic band structure by the result that the three ⟨100⟩ directions are no longer equivalent. Electronic energies along the tensile strain axis are raised, while energies along the directions in compression are lowered.[26]

At the zone center, strain lifts the twofold degeneracy of the uppermost valence band, creating an oblate spheroid energy surface and a lower-lying prolate spheroid surface.[4] For the sample geometry used in all of our experiments, this means that the "heavy-hole" state is raised in energy relative to the "light-hole" state. The effects of strain on the band structure are shown schematically in Fig. 4. The band-structure diagram shows energies along the two nonequivalent ⟨100⟩ axes. The magnitude of the strain is so large that the lowest-lying energy level even in pure Ge will be formed from the $X_{\parallel}$ states instead of L states. In the case of a superlattice consisting of alternating layers of unstrained Si and strained Ge, the minimum of the conduction band lies in Si because of the large band offset between Si and Ge. Because the top of the strain-split valence band of Ge is nearly 0.8 eV above that for strain-free Si,[27] ⟨100⟩ minima in Si lie below the strain-split Ge conduction-band edge. It should be noted, however, that if the sign of the strain is reversed by the growing pure Si on a Ge substrate, then the $X_{\parallel}$ states in Si would be in tension, and the lowest-lying conduction-band states would be formed from the Si ($X_{\perp}$) states in compression that lie along the superlattice direction. This simple observation illustrates the important effect that the substrate lattice constant and orientation have on strain-related modifications of the electronic band structure.

IV. EXPERIMENTAL RESULTS

A. (1:1) Ge-Si superlattice

The (1:1) atomic monolayer superlattice was grown for 16 periods. The total thickness of the structure is 46 Å. The compositional modulation between Si and Ge is imposed only along the [001] growth direction. The resulting superlattice is identical with the three-dimensional zinc-blende structure of GaAs. As such, the (1:1) superlattice does not have inversion symmetry, and is unique in this regard among all of the structures reported in this work.

Local-density-functional calculations by Froyen *et al.*,[9] have been performed on the (1:1) superlattice in which the compositional modulation takes place on a scale much smaller than the unit-cell dimension. The results show little difference from that of a random alloy of 50% Si–50% Ge. The electroreflectance spectrum for this superlattice is shown in Fig. 5. The spectrum shows six features. Those labeled 1 through 3 can be identified with the E_1-E_0' complex of Si. They are common to all the spectra measured in our study. Because there are no optical transitions in Si that occur at energies less than 3.2 eV, all of the other spectral features in Fig. 5 come from the 46-Å superlattice region.

The electronic state energies have been calculated using the envelope-function approximation to treat the 46-Å Ge-Si region as a single quantum well. The effects of strain are calculated from the strain-dependent Hamiltonian used in our previous work on strained alloy quantum wells.[4] This procedure allows us to estimate the expected transition energies for a strained random alloy. These are as follows:

Composition and strain		Quantum confinement
$E_0(1)=2.52$ eV	+	0.05 eV
$E_0(2)=2.62$ eV	+	0.11 eV
$E_0+\Delta_0=2.87$ eV	+	0.1 eV
$E_1=2.82$ eV	+	0.03 eV
$E_1+\Delta_1=3.14$ eV	+	0.03 eV

One-dimensional quantum confinement by the 46-Å superlattice will increase these energies as shown above. This effect is most pronounced on the complex of E_0 transitions because of the relatively low electron effective mass at Γ. In Table II we give the transition energies and linewidths obtained by fitting the line-shape function to the data shown in Fig. 5.

Relatively good agreement exists between these theoretical calculations and experiment for the energies of the E_0 transitions. In particular, the $E_0(1)$ transition at 2.60 eV is the lowest bulk transition energy for the

three-dimensional random alloy. When this value is compared to the corresponding level for ordered superlattices, it will be seen that the transitions for the ordered structures occur at significantly lower energies.

The calculated energy for the E_1 structure occurs at 2.85 eV. The corresponding experimental feature, however, lies at 2.92 eV, which appears to be higher than theory. Given the good agreement between theory and experiment for the E_0 transitions, this discrepancy may warrant explanation. Note that the measured linewidth is twice that for the E_0 transitions. This suggests the presence of an additional transition near 2.9 eV. Although not resolved in experiment, the $E_0+\Delta_0$ transition is expected near 2.97 eV, and we explain both the width and energy position of the 2.92-eV feature by the overlap of the E_1 and $E_0+\Delta_0$ transitions. A strain splitting between the E_1 and $E_1+\Delta_1$ transitions of 0.20 eV is expected and a corresponding feature is measured at 3.18 eV.

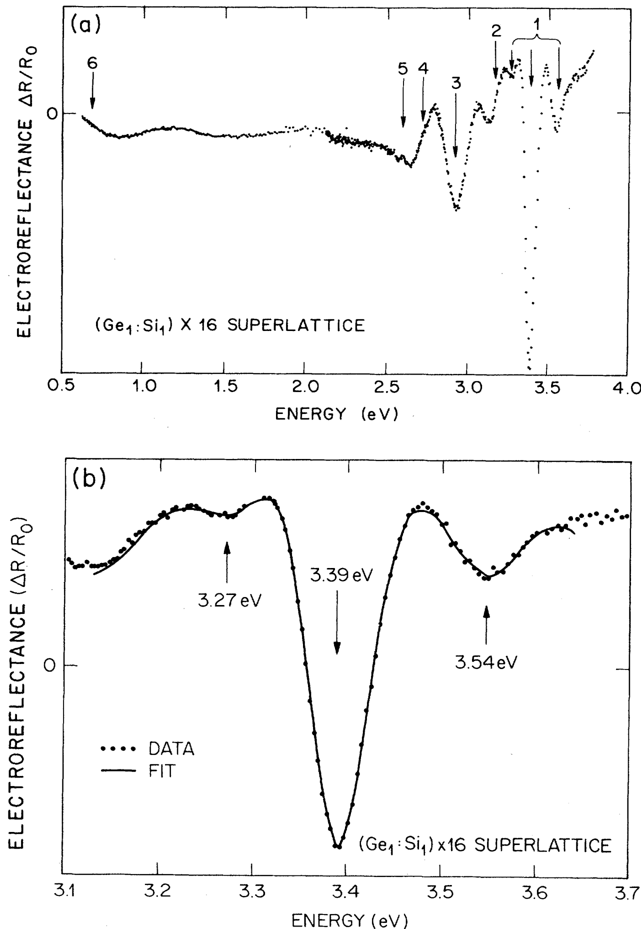

FIG. 5. (a) Electroreflectance spectrum of a (1:1) Ge/Si atomic monolayer superlattice grown on (100) Si. Total superlattice thickness is 46 Å. The spectrum shows Si-related features near 3.4 eV. The remaining transitions at lower energy all originate in the 46-Å superlattice region. (b) Results of line-shape fitting near 3.5 eV, corresponding to the Si E_1-E_0' transitions.

In brief, the measured energy levels of the (1:1) superlattice agree within 0.1 eV with those expected for a random alloy. As we have shown in earlier work,[4] there is also good agreement between experimental values for the critical-point energies and theoretical values calculated by using a strain-dependent Hamiltonian and bulk values for elastic constants and lattice parameters.

There is one additional feature in the spectrum—at lower energies—that bears comment. It is a relatively wide feature centered at 0.68 eV. This energy coincides with the indirect gap of a strained Ge-Si (Ref. 3) alloy of the same composition. The observation of an indirect edge in electroreflectance is not normally expected because of the much smaller optical matrix element for indirect transitions. However, indirect features have been resolved in electroreflectance studies of $Al_xGa_{1-x}Sb$.[28] We expect such features to be more difficult, but not impossible to see in our measurements. Our ability to resolve such features is due to improved resolution of the experimental setup, and in particular, to the longer averaging time made possible by digital recording. We, therefore, attribute this feature to the indirect band gap of the alloy.

B. (2:2) Ge-Si superlattice

The (2:2) atomic monolayer structure was grown for ten periods; the entire structure is 56 Å wide. The (2:2) ideal superlattice has a center of inversion symmetry and a tetragonal unit cell. The primitive unit cell of this structure consists of two atoms of Si and two atoms of Ge in the superlattice direction. Appealing to the simplified notion of "zone folding," the Brillouin zone of this structure is "folded" once along the superlattice direction. Although the Brillouin zone is not "folded" along the two mutually orthogonal directions in the plane of the superlattice, the band structure is, nevertheless, modified along these directions. Portions of the band structure with a k_z component near the edge of the Brillouin zone will be projected onto the $\langle 100 \rangle$ and $\langle 010 \rangle$ $k_\parallel$ directions in **k** space. The in-plane lattice parameter of the unit cell is 5.43 Å, fixed by the Si substrate. Perpendicular to the substrate plane, the lattice parameter is calculated to the 5.62 Å based on bulk elastic constants of Ge. However, the actual distortion of the Ge sublattice cannot be accurately measured by conventional means. Unlike the (1:1) structure, all the strain is concentrated principally in the Ge bilayers and the interface bonds instead of being distributed uniformly through the structure.

The electroreflectance spectrum for this sample is shown in Fig. 6. First of all, the characteristic triplet for the Si E_1-E_0' complex can be seen near 3.4 eV, just as in Fig. 5. Lying at lower energies is a series of transitions, giving a spectrum that is richer than that of the (1:1) superlattice. The $E_0(1)$ and $E_0(2)$ transitions are centered near 2.3 eV, nearly 200 meV lower than their position in the (1:1) structure. This difference in energy for a structure of the same average composition is directly attributable to the presence of superlattice-induced minibands that are present in this structure, but absent in the (1:1) superlattice. While this point will be covered in some detail in the discussion of our results, it can be pointed out

TABLE II. Properties of the principle optical transitions for a (1:1) superlattice.

Peak no.	Energy (eV)	Amplitude ($\Delta R/R_0$)	Linewidth (eV)	Origin	Transition energy for $Ge_{0.5}Si_{0.5}$ alloy (eV)
1	3.54	3.6×10^{-4}	0.11	Si	3.55
	3.39	7.1×10^{-4}	0.08	E_1-E_0'	3.40
	3.27	1.0×10^{-4}	0.08	complex	3.30
2	3.18	2×10^{-4}	0.11	$E_1+\Delta_1$	3.17
				$E_0+\Delta_0$	2.97
3	2.92	9×10^{-4}	0.12	E_1	2.85
4	2.72	2×10^{-4}	0.12	$E_0(2)$	2.73
5	2.60	1×10^{-4}	0.13	$E_0(1)$	2.57
6	0.68	$\sim10^{-6}$	0.20	E_g	Indirect gap at 0.7 eV

briefly here that the lowest-energy miniband created by the superlattice potential is expected to lie lower in energy than the virtual-crystal energy of the random alloy for these structures. Our measurements for the (2:2) structure are summarized in Table III.

The superlattice potential splits the E_1 and $E_1+\Delta_1$ transitions into six which have nonzero matrix elements.[12] The two main features can be seen at 2.78 and 2.93 eV. Some of the higher-lying E_1-related structure is resolved at 3.11 eV. This splitting reflects the presence of the superlattice: the E_1 states are projected onto the two-dimensional zone parallel plane, and along the one-dimensional superlattice direction. Superlattice induced mixing of this state produces additional levels, only some of which are resolved in our measurements.

Strain alone cannot produce this effect because a ⟨001⟩ uniaxial strain affects all the energy levels with [111] symmetry in exactly the same way. The observed splitting is expected to occur when the superlattice period is short enough to modify the cubic symmetry of the Brillouin zone.

C. (4:4) Ge-Si superlattice

The (4:4) structure consists essentially of alternating cubic cells of Si and Ge in the [001] direction. The entire superlattice structure that we studied is 52 Å wide and consists of five periods of four monolayers of Si alternating with four monolayers of Ge. In this case, the primitive unit cell consists of eight atoms, and the Brillouin zone is folded twice along the superlattice, but still remains unfolded in the superlattice plane. This gives a square "pillbox" geometry to the Brillouin zone in **k** space rather than the truncated octahedron that is the case for fcc semiconductors. A transmission electron micrograph showing the lattice-resolved image of this structure is shown in Fig. 7. This image provides direct evidence for extended layering.

Original theoretical studies of this superlattice were made by Gnutzmann and Clausecker, who modeled the band structure using the concept of folding of the Brillouin zone and the envelope-function approximation.[29] In this work, it was demonstrated that the amplitude of a transition between the valence-band maximum and a zone-folded band at Γ could be as large as 10% of that for a direct optical transition. This approach was further developed by Moriarty and Krishnamurthy, who derived the form of the band structure for the Ge/Si (4:4) superlattice.[30] Additional theoretical studies of this superlattice were made by Van de Walle and Martin in order to

TABLE III. Properties of the principal optical transitions for a (2:2) superlattice.

Peak no.	Energy (eV)	Amplitude ($\Delta R/R_0$)	Linewidth (eV)	Origin	Remarks
1	3.52	5×10^{-6}	0.08	Si	
	3.38	1.4×10^{-5}	0.07	E_1-E_0'	
	3.30	1×10^{-6}	0.09	complex	
2	3.11	2.4×10^{-6}	0.13		
3	2.93	9×10^{-5}	0.10	$E_1^{\perp}$	doublet
4	2.78	1.4×10^{-4}	0.09	$E_1^{\parallel}$	
5	2.41	3.9×10^{-4}	0.24	$E_0(2)$	splitting of valence
6	2.21	4.2×10^{-5}	0.18	$E_0(1)$	band is equal to 0.20 eV
7	0.85	$\sim1\times10^{-7}$	0.3	E_g	resolution of indirect band gap

determine the valence-band offset between Si and Ge.[27] Experimental measurements have confirmed these calculations.[31] Evidence from Shubnikov–de Haas oscillations on n-type samples support the results of these studies by showing a very small conduction-band offset.[32,33] In the work of van de Walle and Martin, it was shown that the bulk atomic potentials of Si and Ge were well established in only two atomic monolayers. The unit cell of the synthetic crystal formed by the superlattice is shown in Fig. 1(b). People and Jackson used the results of Van de Walle and Martin to derive the electronic energy levels of the (4:4) structure in a Kronig-Penney approximation. The strength of this approach lies in its simplicity. In applying this method, it should be noted that the Brillouin zone experiences an additional folding to that shown in Fig. 1 of Ref. 10, the effect of which is to introduce an additional level at the zone center near 1.7 eV. The generally good agreement between the critical-point energies

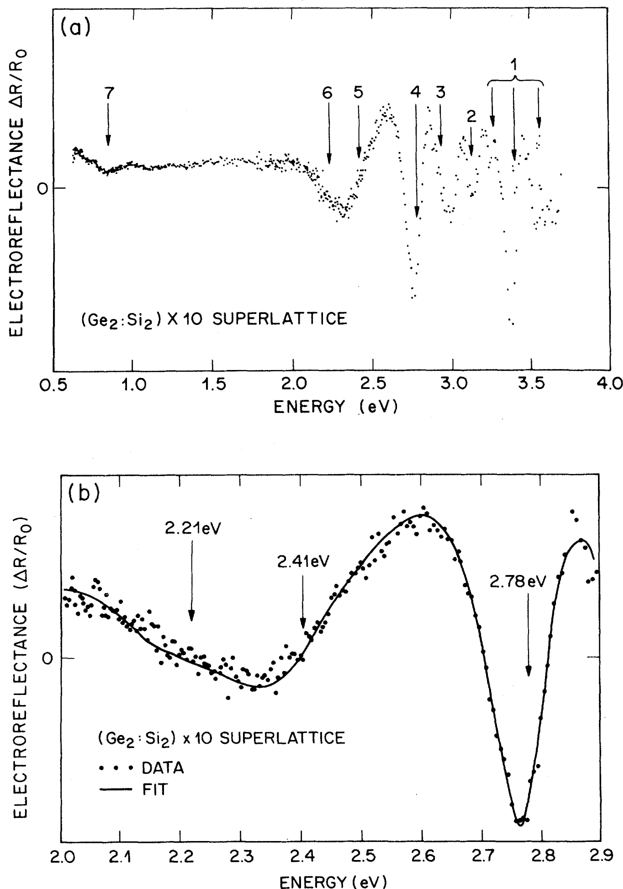

FIG. 6. (a) Electroreflectance spectrum of a (2:2) Ge/Si atomic monolayer superlattice grown on (001) Si. The broad feature near 2.3 eV is derived from the E_0 transition in a strained random alloy. Its appearance at 2.3 eV instead of 2.6 eV is the result of the superlattice structure. (b) Line-shape fitting of the (2:2) structure in the vicinity of the E_0 transition. The valence-band splitting of 0.2 eV is resolved by the fitting procedure.

by this method when compared to results from other more fundamental theoretical approaches establishes an *a posteriori* justification for the validity of an envelope-function model in this thickness regime.[10,12,34] This agreement also lends support to the notion that in addition to bulk potentials being well established in the superlattice, as Van de Walle and Martin have shown, bulk energy levels of Si and Ge are also well established in the (4:4) structure.

The electroreflectance spectrum of the (4:4) structure is shown in Fig. 8. The triplet of states near 3.4 eV, related to the E_1 and E_0' transitions in bulk Si is clearly resolved. Below 3.2 eV there is a rich spectrum of transitions coming from the superlattice structure itself. Near 2.8 eV, the E_1 and $E_1+\Delta$ transitions are split into multiple components labeled by the arrows 2, 3, 4, and 5. Peak 5 is a doublet. The superlattice-induced splitting, first resolved in the (2:2) spectrum, is now well developed. Microscopic band-structure calculations for this superlattice support our observations in some detail.[9,12] These transitions are resolved in our spectra at peak 2 (3.22 eV), peak 3 (3.04 eV), peak 4 (2.82 eV), and peak 5 (2.58 and 2.61 eV). The splitting of the E_1 transition is the signature of the result that the electronic states reflect the noncubic superlattice symmetry rather than the cubic symmetry of a homogeneous alloy. In more precise terms, the splitting of the E_1 transition is due to the breaking of the C_4 symmetry along the growth axis.

The E_0-derived transition for this structure occurs near 2.3 eV. The E_0 transition is split into two components because the cubic symmetry is broken by strain and superlattice geometry. The presence of two components to the E_0 transition is seen in the width of the feature. The energy positions of these two components can be determined more precisely by line-shape analysis of this feature. As in the case of the (2:2) superlattice, the observation that the E_0 feature lies much lower in energy than the virtual-crystal average of Ge and Si is expected, because the electronic states at the zone center reflect the presence of a superlattice rather than an alloy.

Below 2.0 eV, an additional series of transitions is resolved in the (4:4) superlattice structure. Two of these transitions at 0.8 and 1.3 eV were clearly visible in Fig. 8. We have previously identified these new features as structurally induced optical transitions. Experimentally, these transitions have an amplitude similar to that of the direct optical transitions lying at higher energies.

The appearance of additional direct optical gaps might be expected in the superlattice, because the periodic potential will mix zone-edge and zone-center states, creating additional bands at the zone center. All theoretical calculations done so far show new gaps appear whose energies correspond closely to those measured here. However, the character of these new gaps in either indirect or quasidirect. In an extended superlattice the transition matrix element associated with these structurally induced transitions should be quite small, and the measured amplitude should be similar to that seen in the (1:1) or (2:2) superlattices near 0.8 eV; that is, about 2–3 orders of magnitude less than that for a bulk direct optical transition.

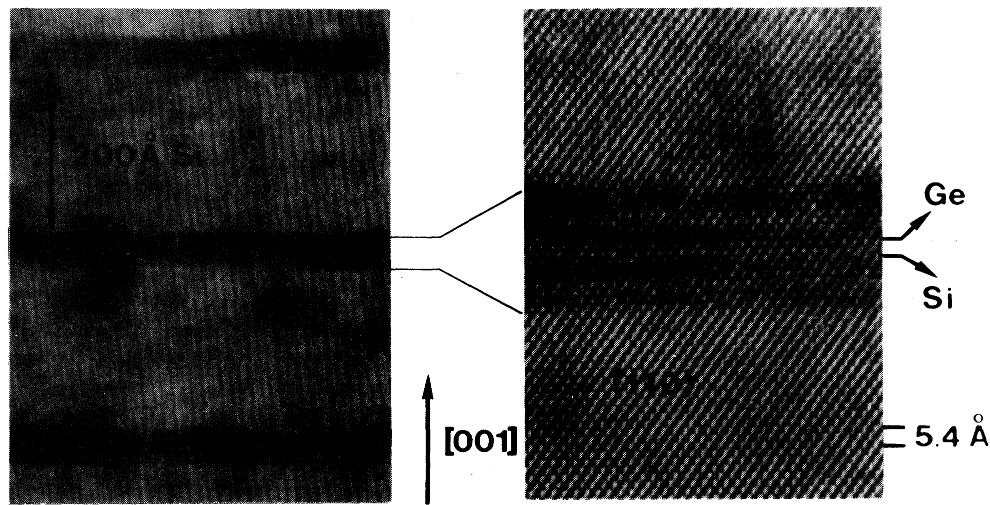

FIG. 7. Transmission micrograph of an extended (4:4) superlattice grown by MBE. Direct lattice imaging is used to resolve pairs of atoms. The lower-magnification cross section of the sample shows that planarity is maintained both laterally and in the growth direction.

In Table IV we have listed the measured transition energies for the (4:4) structure. We have also listed the results of calculations of the expected energies for this superlattice. The agreement between calculations and experiment is very close. Furthermore, the good agreement for the transition energies between the results, first-principles theory, and the Kronig-Penney envelope-function approximation gives some support to the notion that the electronic levels in the (4:4) superlattice are determined largely by the energy levels of bulk Si and Ge. This result differentiates the (4:4) superlattice from the (2:2) superlattice, where the measured energy levels cannot be so simply deduced from levels in bulk Si and Ge.

In reporting the results shown in Table IV, we note that the 1.70-eV transition was seen clearly in one sample,[35] but was resolved weakly in the sample whose spectrum is shown in Fig. 8. Appeal to the envelope-function approximation shows that one component of this transition arises from the double folding of the Brillouin zone from the eight-atom periodicity. The missing 1.70-eV feature may be an indication of the absence of longer-range order.

TABLE IV. Principal optical transitions for a (4:4) superlattice. Results are compared to some calculated values for the optical transition energies.

Trans. no.	Energy (eV)	$\Delta R/R$ ampl.	Linewidth (eV)	Origin ident.	First-principles band struct. (eV) (a)	Local-density approx. (eV) (b)	Kronig-Penney envelope-function approx. (eV) (c)
1	3.56	2×10^{-3}	0.08	Si	3.56		
	3.39	7×10^{-3}	0.08	E_1-E_0'	3.40		
	3.29	2×10^{-4}	0.07	complex	3.31		
2	3.22	4×10^{-4}	0.07	$E_1+\Delta_1^{\perp}$	3.26		
3	3.04	1.8×10^{-4}	0.06	$E_1+\Delta_1^{\parallel}$	3.18		
4	2.82	1.6×10^{-3}	0.11	$E_1^{\perp}$	2.88		
5	2.60	2.1×10^{-3}	0.13	$E_1^{\parallel}$ (doublet)	2.54		
					2.50		
6	2.38	5×10^{-3}	0.22	E_0 (doublet)	2.41		
	2.20	2×10^{-3}	0.25		2.20	2.3	2.41
7	1.70	5×10^{-5}	0.20	zone folded (quasidirect)	1.76	1.9	1.7
8	1.25	5×10^{-5}	0.20	zone folded (quasidirect)	1.24	1.2	1.20
9	0.76	3×10^{-5}	0.20	E_g (indirect)	0.85	0.8	0.84

[a]Reference 12.
[b]Reference 29.
[c]Reference 10.

V. DISCUSSION

In our experiments we have investigated a series of superlattices which have a similar average composition, close to $Ge_{0.5}Si_{0.5}$, and a similar thickness, 50 Å. This series of structures forms a convenient framework for following the evolution of the electronic band structure from that of a random alloy to that of a multiple quantum-well structure in which the potential wells and barriers are formed by materials with well-defined bulk values.

Our clearest experimental observation is that some of the ordered samples used in this study have measured electronic energy spectra that are quite distinct from that of a random alloy. In our discussion we consider the possible origin of this new structure, the relationship between our measurements and theoretical calculations of the electronic structure, and important differences between the ideal superlattices treated in theory and the actual conditions under which experimental data were taken.

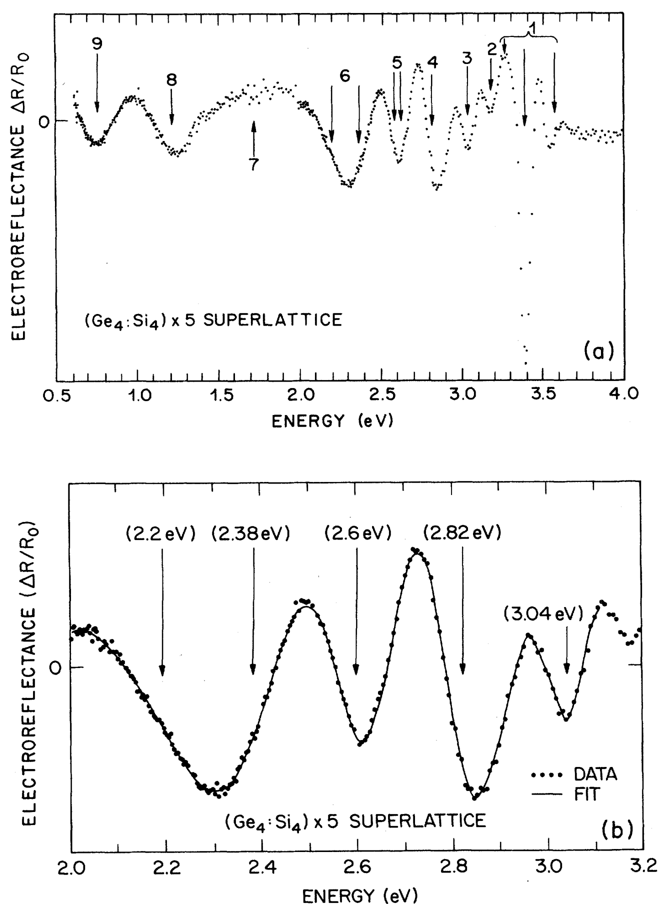

FIG. 8. (a) Electroreflectance spectrum of a (4:4) Ge/Si atomic monolayer superlattice grown on (001) Si. The total superlattice thickness is 52 Å. Prominent peaks in the electroreflectance spectrum at 0.8 and 1.2 eV identify two new structurally induced transitions. (b) Line-shape-fitting results for five transitions between 2.0 and 3.0 eV.

Electroreflectance is an optical characterization technique whose usefulness and accuracy has been well established in many bulk semiconductors and multiple-layer semiconductor heterostructures.[19,36–39] As an optical technique, electroreflectance is sensitive to extended electronic states rather than localized defects.[39] Our experimental measurements sample a macroscopically large surface area, and resolution of distinct transitions depends on sample uniformity over the better part of 0.1 cm^2. The measurement of new optical transitions in an ordered Ge/Si superlattice is strong supporting evidence that these transitions occur between new extended states in the valence and conduction bands, as opposed to transitions between defect states introduced by vacancies, dislocations, or impurities.

A. Comparison of theories with experimental results

We are aware of at least five different theoretical approaches to the calculation of the electronic band structure of ordered Ge/Si superlattices: local-density-functional approximation,[9,13,34] empirical pseudopotential,[15] tight binding,[38,40] envelope-function approximation,[10] and quasiparticle calculations.[12,35] In all of these investigations, the Ge/Si superlattice is treated as an ideal structure of infinite extent with perfect interfaces. The measurements are made, however, on nonideal structures under somewhat different conditions. The most important of these are listed briefly.

(1) *Electric field.* Electroreflectance requires an applied electric field to modulate the transition energy. In our case, the electric field is applied along the superlattice axis and creates a symmetry-breaking potential.

(2) *Limited extent of the superlattice structure.* In the (4:4) superlattice, five superlattice periods can be grown before the critical thickness limit is reached. The assumption of infinite spatial extent permits the use of periodic boundary conditions in a calculation, but important edge effects may be present in experiment.

(3) *Interface roughness.* The transmission-electron-microscopy (TEM) micrograph that we have shown in Fig. 7 could be used to estimate that the interface roughness in a (4:4) superlattice is about ±1 atomic monolayers. This represents a stunning achievement for molecular-beam-epitaxial (MBE) growth technology. On the other hand, an uncertainty of ±1 atomic monolayer translates into variations in the (4:4) superlattice structure that are 50% of the nominal thickness. For the (2:2) ordered structure, a fluctuation of this magnitude has even more dramatic effects on the sample structure. Hence, interfacial roughness can be expected to be an important perturbation. For similar reasons the presence of dislocations may also be a factor in disturbing translational symmetry.

B. Superlattice ordering in the atomic monolayer structures

In studies of the electronic band structure by Froyen *et al.*,[9,32] it has been seen that the electronic structure of the (1:1) superlattice appears to differ only slightly from that of a random alloy. For the critical points measured in

our electroreflectance experiments, no differences between the two are expected. In addition, our observations of interfacial roughness in (4:4) structures lead us to conclude that extended, long-range layering appears unlikely in the (1:1) structure. The analysis of our electroreflectance data, in fact, shows the energy spectrum of the (1:1) sample to resemble that obtained from a random alloy of similar average composition. These spectra are quite distinct from those for the ordered (4:4) structure shown in Fig. 8.

In our measurements, we characterized an additional structure: (6:6) Ge/Si on (001) Si. Six monolayers of Ge grown on Si are close to the critical thickness limit.[5] The superlattice consisted of three periods, and following Hull's rule[41] it is likely that the critical thickness limit was exceeding during the growth of the second layer of Ge. The electroreflectance spectrum of this sample is shown in Fig. 9, and it is compared to the (1:1) superlattice and a random alloy of a similar composition. It can be seen readily that the (1:1) and (6:6) spectra are very similar to each other. These two spectra are closely related to that for the random alloy with the primary difference being the precise position of the E_1 transition. All three samples display the common feature that there are no significant optical transitions measured below 2.5 eV.

The comparison shown in Fig. 9 suggests that the (6:6) superlattice structure lacks extended long-range order. TEM examination of this (6:6) structure has shown this conjecture to be the case. Figure 10 is a lattice image of a three-period (6:6) Ge/Si sample. Layering is observed for the first Ge deposition, but the second and third layers

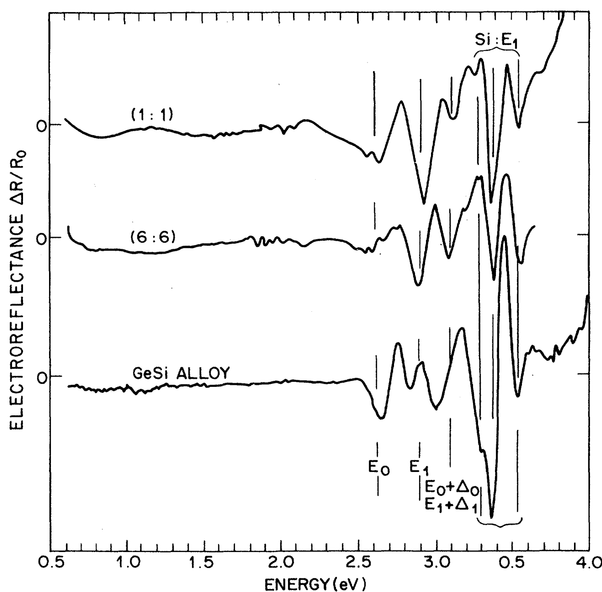

FIG. 9. The electroreflectance spectra of a (6:6) Ge/Si structure, a (1:1) structure, and a strained $Ge_{0.45}Si_{0.55}$ alloy. These three spectra are quite similar, supporting the conclusion that the (1:1) and (6:6) structures have an alloylike electronic band structure.

display disorder manifested by irregularities in thickness, as well as the presence of defect clusters and dislocations. These results show that six monolayers of Ge are very close to the "critical thickness" for the pseudomorphic defect-free growth of Ge on Si, and that further deposition of Ge exceeds this value, giving rise to strain relaxation. This relaxation prevents strong layering of subsequently deposited Ge.

These results show that electroreflectance can be used as an effective tool for measuring the presence of superlattice ordering on an atomic scale. Our results on the (6:6) structure show alloylike behavior that is confirmed by TEM analysis. In addition, electroreflectance measurements have shown similar alloylike behavior for the (1:1) structure where other methods of structural characterization such as TEM or x-ray diffraction can no longer be used.

The electroreflectance spectra of the (2:2) and (4:4) structures show significant departures from that of the (1:1). A comparison of these three measurements is shown in Fig. 11. There are two principal features that distinguish the ordered superlattices from the (1:1) structure. One is the presence of a strong superlattice transition at $\sim$2.3 eV that does not appear in the (1:1) structure. The second is the richness of the electroreflectance spectra of the superlattice samples between 2.5 and 3.0 eV compared to that of the (1:1).

The ideal (1:1) Ge/Si superlattice is identical in structure to bulk GaAs; that is to say, it is in fact a zinc-blende structure rather than a superlattice. The electronic structure of the ideal (1:1) ordered structure is expected to resemble that of a compound material closely related to a Ge-Si alloy, with small splittings related to the difference in atomic potentials between Si and Ge. Experimental results on the (1:1) structure are consistent with this expectation, but our results could be explained as well by lack of ordering as by formation of the intended zinc-blende structure.[42]

For structures larger than the (1:1), e.g., (2:2), a superlattice is formed. A superlattice is also formed by the (4:4) structure. While the (6:6) structure would be an interesting superlattice to study, we have seen that the constraints imposed by lattice-mismatch strain do not permit the commensurate growth of this structure on (001) Si.

Creating a superlattice structure with distinct electronic properties depends on two important considerations. One is the creation of extended well-defined layering in the plane of the superlattice. The implications and limits of this requirement have already been discussed. A second important consideration is that the number of superlattice periods must be sufficient for electrons to "sense" the presence of a superlattice. In our experimental work, the number of periods that are permitted is strictly limited by strain. In the case of the (2:2) structure, ten periods can be grown. For the (4:4), the limit is five. As we have seen in the case of the (6:6) structure, only one period can be grown pseudomorphically on Si.

One of the most interesting fundamental issues raised by our experiments is concerned with this second consideration. While we have not yet performed systematic experiments to determine the dividing line between a su-

perlattice and a defect plane, we have observed that five periods of the (4:4) structure are sufficient to form a superlattice whose characteristic energy levels are reproduced closely by calculations that assume an infinite number of periods. It would appear, therefore, that five periods is an upper bound, at least for Ge/Si structures, for the required number of periods for superlattice formation.

C. Superlattice formation and the envelope-function approximation

The electronic wave function in a crystal is composed of two parts: (a) states that depend on the local atomic environment and the symmetry of the lattice, and (b) plane-wave states. The Kronig-Penney model of electronic states in a crystal makes this distinction quite explicit. The dispersion equation is expressed as

$$\cos(qd)=\cos(k_w l_w)\cosh(k_b l_b) + A\sin(k_w l_w)\sinh(k_b l_b)\ , \tag{3}$$

where $l_w + l_b = d$, the superlattice period.

Contained in A are parameters that depend only on the energy-level structure of the constituent materials involved in superlattice formation.

If the period of the superlattice is reduced to its lower limit of two planes of atoms, the Kronig-Penney model averages the potentials associated with the "well" and "barrier" regions, and is independent of any other features of the band structure contained in A, and, therefore, whether bulk band structures exist for the monolayer Ge and Si regions in such a case is unimportant.

This result can be derived simply in the effective-mass approximation using the condition of conservation of particle current at the superlattice boundary. In the limit that $d \rightarrow 0$, with $l_w = l_b$, one obtains to second order

$$k_w^2 - k_b^2 + \frac{m_b}{m_w}k_w^2 - \frac{m_w}{m_b}k_b^2 = 0\ , \tag{4}$$

and, recalling that $k_w^2 = 2m_w E$ and $k_b^2 = 2m_b(V_0 - E)$, Eq. (4) immediately simplifies to

$$E = \tfrac{1}{2}V_0\ , \tag{5}$$

and is independent of features of the band structure which, in this model, are represented by effective mass.

This line of reasoning supports the notion that the (1:1) superlattice should have an energy-band structure that tends to approach that given by the average of the band structures of Ge and Si, and shown in Fig. 4. In particular, it implies that the lowest-energy optical transition, labeled E_0, should occur at the virtual-crystal value of 2.6 eV, for both the alloy structure and the (1:1) superlattice. This conclusion is in excellent agreement with experiment for these samples.

For a superlattice period of eight atomic layers, (4:4), the situation is quite different. The work of Van de Walle and Martin established that bulk atomic potentials for Ge and Si are well established in the barrier and well regions. The method used by People and Jackson can be used with bulk band-structure parameters of Ge and Si to evaluate the Kronig-Penney model [Eq. (3)] with results that are close to those obtained from first-principles band-structure calculations. One of the important results of this study is that the transition energy for the E_0 transition in the (4:4) superlattice lies at 2.3 eV, significantly below the virtual-crystal value of 2.6 eV, reflecting the effect of the longer eight-atom superlattice period.

The case of the (2:2) structure is intermediate in some respects between these two extremes. The results of the electroreflectance show the clear signature of superlattice formation. The E_1 transition is split into several components, and the E_0 transitions occur at lower energies than the upper limit of the virtual-crystal approximation. The Kronig-Penney model does give bandlike solutions for this period, but the energies can no longer be accurately computed. The failure of the model to give accurate energies in this regime is attributed to the use of bulk band-structure parameters of Ge and Si to evaluate Eq. (3). In fact, each Ge atom has one Si and one Ge atom for nearest neighbors along the superlattice direction. The symmetry-related components of the Kronig-Penney model, however, appear to behave correctly; that is, solutions are obtained for superlattice bandlike states in agreement with experiment. A schematic diagram of this evolution is shown in Fig. 11, where we compare the spectra of superlattice samples to the (1:1) structure.

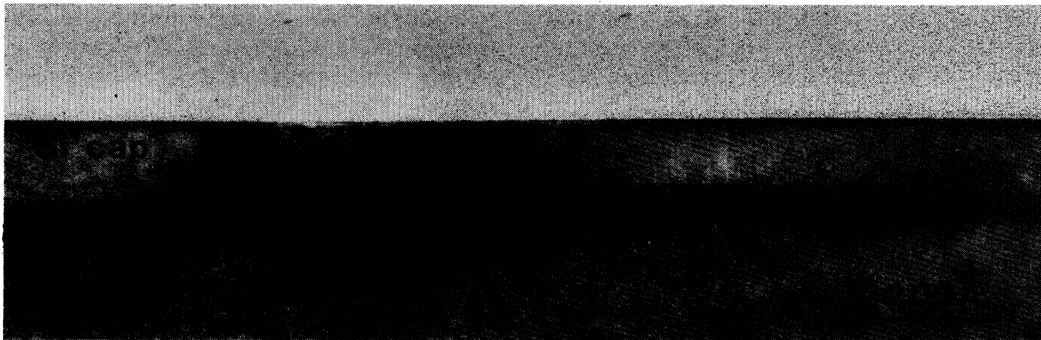

FIG. 10. TEM cross section in the lattice-imaging mode of the (6:6) superlattice structure. The critical thickness limit was exceeded during growth, resulting in an absence of long-range coherent layering of Ge and Si.

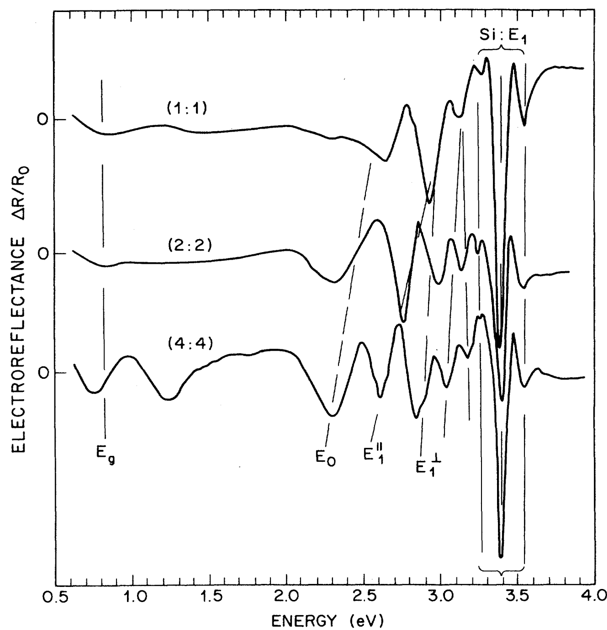

FIG. 11. Electroreflectance spectra of (1:1), (2:2), and (4:4) superlattice structures showing the evolution from an alloy band structure to a superlattice formed by bulklike Ge and Si.

Deviation from the Kronig-Penney results obtained using bulk band-structure values from those obtained in experiment can be most easily seen in the (2:2) structure for the E_0 transition. The Kronig-Penney solution puts this transition energy near 2.5 eV; experiment is close to 2.3 eV. The presence of the E_0 level clearly below the virtual-crystal value of 2.6 eV means that a superlattice has been formed between different band structures. The discrepancy between calculation and experiment in the case of the (2:2) superlattice indicates that there are significant departures from bulk levels of Ge and Si in the (2:2) superlattice.

D. The character of the fundamental band gap

The initial electroreflectance spectroscopy studies of Ge/Si superlattices revealed the presence of reproducible optical transitions, the amplitudes of which are comparable to those of *bona fide* direct optical transitions. Of course, the presence of direct optical transitions (such as the 3.4-eV transition in Si or the 0.8-eV transition in Ge) does not mean that the fundamental band gap is direct in character.

In the case of Ge/Si superlattices grown on (001) Si, the presence of new optical transitions in the infrared might prompt speculation that the superlattice would have a fundamental band gap that is also direct in character. In the case of the Ge/Si (4:4) superlattice, where the potentials of the Ge and Si regions are closely approximated by bulk values, it can be seen readily that the lowest-energy state in the conduction band is formed from Si band-edge states lying along directions parallel to the planes of the superlattice.[9–13] The band-edge states of Si that lie along the superlattice direction are folded twice with respect to the center of the Brillouin zone, but they lie higher in energy than the conduction-band minima near the (010) and (100) zone boundaries. Thus, the superlattice is an indirect-band-gap material.

The large band offset between the valence bands of Si and Ge, $\Delta E \simeq 0.8$ eV, is responsible for the type-II nature of the superlattice. The valence-band maxima lie in Ge and the conduction-band minima lie in Si. Although the quantitative details change from structure to structure, two basic features of ordered Ge/Si superlattices on (001) Si are constant: (1) the large valence-band offset gives a type-II alignment, ensuring that the conduction-band minima are formed from Si states, and (2) the superlattice periodic potential creates states at the zone center whose energies are above that for the nonfolded minima that lie parallel to the plane of the superlattice.

The transition matrix elements for the series of superlattices considered in this paper have been computed by several groups.[9,11,12,15] There are four optical transitions that are measured between 0.7 and 2.5 eV in the (4:4) structure. Taking the measured amplitude of the transition near 2.3 eV as unity, we can compare measured amplitudes with the square of the calculated matrix elements. These are shown in Table V.

This comparison shows that measured transition amplitudes tend to be larger than values expected by comparison of calculated matrix elements. However, the lowest-energy optical transition at 300 K occurs at 1.0 eV and is forbidden by symmetry. Experimentally, a strong transition is observed at 0.76 eV, quite close to the indirect-band-gap energy calculated for this superlattice.

On the basis alone of the transition *energy*, one would conclude that the electroreflectance measurement had resolved the indirect band gap. However, the amplitude for such a transition should be small, about 10^{-3} less than that for direct transitions. In fact, we have successfully resolved indirect transitions in Ge-Si bulk alloys and measured transition amplitudes are weaker by about this amount.

Aside from discarding the experiment or the theory, it appears that the resolution of this apparent conflict may lie in the differences between conditions under which measurements were made, and in the assumptions upon which the calculations have been based. As a result, it is not possible to determine from our experiments the character of the lowest-lying transition in this superlattice. The distinction of direct or indirect transition may not be entirely useful for structures of the dimensions of our samples. Measurement shows that the transition amplitude has been greatly enhanced. It appears that the large electric field and edge effects at the Si/Ge-Si interfaces may play an important role in modifying transition amplitudes.[43] These differences mean that some of the properties of an infinite, ideal superlattice are not confirmed in our measurements because experimental conditions represent a significant departure from the ideal case. The implications of this point have been discussed by Wong *et al.*[15] Their calculated oscillator strengths are in somewhat closer agreement with our observations. It is our conclusion that the 0.76-eV optical transition does in-

TABLE V. Comparison between transition amplitudes measured in electroreflectance and some results obtained by calculation. The matrix element and measured amplitude at 2.3 eV have been taken as unity for the purposes of this comparison. The measured amplitude is proportional to the square of the matrix element. Although the calculations vary, they all show that the measured amplitudes for structurally induced transitions should be much smaller than that for the 2.3-eV transitions. The large deviation suggests that features extrinsic to the ideal superlattice band structure may be enhancing the observed amplitudes.

	2.3 eV	1.65 eV	1.2 eV	0.76 eV	Ref.
Measurement amplitude	1.0	0.01	0.01	0.01	
Calculation $\lvert\langle \Upsilon_1 \lvert p \rvert \Upsilon_2 \rangle\rvert^2$	1.0	2×10^{-4}	2.5×10^{-6}	0.0	a
	1.0	2×10^{-3}	2×10^{-4}	0.0	b
	1.0		0.01	4×10^{-5}	c

[a]Reference 29.
[b]Reference 12.
[c]Reference 15.

volve states at the top of the valence band at the zone center and the conduction-band edge along the [010] and [100] directions. Conduction-band states at Γ with an energy of 1.0 eV may also play an important role in the observed enhancement of the transition amplitudes. Optical transitions to these latter levels are symmetry forbidden only in a perfect (4:4) structure. Mixing of these states with the conduction-band-edge states could provide the mechanism for increasing the wave-function overlap between the conduction and valence bands that is necessary to achieve the observed increase in transition amplitudes.

E. Character of the lowest-energy optical transition: conditions for wave-function mixing

All of the Ge-Si structures studied in this work, including the $Ge_{0.5}Si_{0.5}$ alloy, show some structure in the electroreflectance spectrum near 0.7 eV. This energy is quite close to that of the indirect band gap, and in the case of the random alloy sample this is the feature in the calculated energy spectrum that might account for the measured structure seen in electroreflectance and photocurrent spectroscopies. It has been pointed out that electronic transitions may also occur between the top of the valence band in Ge and the conduction band of the bulk Si cladding layers on either side of the superlattice region.[35] The effect of an applied electric field used to make the electroreflectance measurement would be to increase the overlap between these two levels. This possibility is an interesting one and needs to be investigated further. Our experiments on Ge-Si alloys establish (a) that the indirect band gap can be resolved in electroreflectance and (b) that the amplitude of this feature is about 10^{-3} that of allowed direct transitions in the same material. Since the (1:1) and (6:6) superlattice samples are in fact seen to be alloylike in actual structure, it is expected that the 0.7-eV feature in the electroreflectance spectrum should be seen to be as small as that observed in the random alloy sample.

The (2:2) and (4:4) superlattices, however, display characteristics of extended superlattice ordering, and the interpretation of the lowest-energy features around 0.7 eV may be more involved. The experimental results on these two samples show quite different behavior. The amplitude of this feature in the (2:2) case is quite small, similar to that described above for the resolution of the indirect band gap. In the case of (4:4), this feature is a prominent transition with an amplitude at least 2 orders of magnitude greater than that measured for indirect transitions.

In an earlier work, we considered the origin of the strong feature seen in the (4:4) superlattice at 0.7 eV in terms of the results of photoconductive spectroscopy[35] and theoretical calculation.[43] We interpreted the 0.7-eV structure as a resolution of the indirect band gap. In light of the present experiments, we believe that this conclusion is inconsistent with the large transition amplitudes measured only in (4:4) superlattice samples. The transitions measured in electroreflectance do not appear to be the same as well-understood, bulk, indirect gaps. Features in the sample and experiment that might enhance the matrix element of such an indirect transition could be (a) wave-function mixing of zone-edge and zone-center states as the result of steps or imperfections in the plane of the superlattices, (b) wave-function mixing of states at the zone center as a result of the symmetry-breaking effect of the electric field, and (c) electric-field-dependent wave-function overlap of states in the bulk Si cladding layers with states in the superlattice region.

The theoretical calculations of the Ge/Si (4:4) band structure show that the lowest-energy transition at Γ lies at about 1.0 eV, only 200 meV higher than the indirect band gap at 0.8 eV. However, transitions to this level from the valence band are symmetry forbidden under the assumptions of these calculations (periodic boundary conditions, perfect interfaces, no electric field). The first direct transition with a nonzero matrix element occurs at 1.25 eV. The energy band along the $X_{\parallel}$ direction overlaps in energy over a considerable part of the Brillouin zone with the energy band along the superlattice axis $X_{\perp}$. The near degeneracy of these states will lead to mixing of states at Γ with states along $X_{\parallel}$ in the presence of a symmetry-breaking potential. Examples of such pertur-

bations are interfacial steps and imperfections. The mixing of Γ and X states occurs throughout the Brillouin zone with a strength that is determined by the Fourier spectrum of the perturbation in **k** space and the energy-difference denominator between the mixed states.

It has been demonstrated in a convincing manner by Meynadier *et al.*[24] that similar Γ-X mixing plays a determining role in photoluminescence of GaAs/AlAs type-II superlattices. In the experiments of Ref. 24, the energy overlap of Γ and X states can be modified by structural parameters. Its effect on photoluminescence has been directly measured and interpreted as evidence for Γ-X mixing. By analogy with this result, one could propose that the large electroreflectance amplitude measured at 0.8 eV may be evidence of wave-function mixing in Ge-Si (4:4) structures. Symmetry-broken transitions of this type have an absorption coefficient that varies with energy as $E^{3/2}$. The results of photocurrent spectroscopy experiments do not distinguish between an energy dependence of the absorption that varies as E^2, indicating an indirect edge, or an $E^{3/2}$ dependence, indicating a symmetry-broken transition.[35] In criticism of this argument, Γ-X mixing implies that momentum conservation is relaxed. Taken to its extreme, however, Γ-X mixing would imply the loss of translational symmetry, and under such conditions the concept of a band structure would become meaningless.

It remains to consider what relationship such an argument might have with regard to the (2:2) superlattice, for which no such large-amplitude electroreflectance signals are observed near 0.8 eV. A clue to the explanation for this difference may lie in differences in the band structure for the (2:2) and (4:4) superlattices.[9–13] In the case of the (2:2) structure, the band-edge states at $X_{\parallel}$ lie 500 meV lower in energy than the states at the zone center.[9] In the (4:4) case, the situation is different with band-edge states overlapping in energy the states at the zone center.[9,12] Because of the larger energy separation between levels in the (2:2) case, the energy denominator in a perturbation calculation will remain finite, while in the (4:4) case the levels are degenerate.

Although wave-function mixing may help to explain the differences between the (2:2) and (4:4) superlattices it does not appear sufficient in itself to explain the large, measured amplitudes seen in the electroreflectance spectra.

VI. CONCLUSIONS

Systematic measurement of Ge/Si monolayer superlattices by electroreflectance spectroscopy has established the existence of new energy levels created by the superlattice potential. Electroreflectance spectroscopy has been shown to be a sensitive and in some cases a unique tool for determining superlattice ordering on an atomic scale.

Comparison between our experimental results on real superlattices and theoretical calculations on the corresponding idealized perfect structure shows excellent agreement on the energies of extended electronic states in these atomic layer superlattices. This agreement is our most eloquent support for the notion that it is now possible to create artificially structured materials with an electronic band structure that can be tailored to some degree during crystal growth. While our experiments were carried out using Ge and Si, extension of this principle to other materials systems is immediate without further qualification.

Significant differences between experiment and theory can be seen in comparison of optical transition matrix elements involving structurally induced electronic states. The measured amplitudes of transitions near the indirect band gap in Ge/Si (4:4) superlattices are much greater than expected from theoretical estimates. While it is plausible to consider structural deviations from an ideal superlattice or external electric field effects as possible causes of a large enhancement in transition amplitudes, further measurement and calculation will be required to confirm quantitatively the presence and importance of these effects on the optical energy spectra.

ACKNOWLEDGMENTS

The authors express their gratitude to the theorists whose study of these materials and open communication of results have stimulated our experimental studies and analysis: P. Friedel, S. Froyen, M. Hybertsen, S. A. Jackson, M. Jaros, R. M. Martin, R. People. S. Satpathy, M. Schlüter, and A. Zunger.

[1]G. Abstreiter, K. Eberl, E. Freiss, W. Wegscheider, and R. Zachai, in Proceedings of the Fifth International Conference on Molecular-Beam Epitaxy, Sapporo, Japan, 1988 (unpublished).

[2]H. Temkin, T. P. Pearsall, J. C. Bean, R. A. Logan, and S. Luryi, Appl. Phys. Lett. **48**, 963 (1986).

[3]D. V. Lang, R. People, J. C. Bean, and A. M. Sergent, Appl. Phys. Lett. **47**, 1333 (1985).

[4]T. P. Pearsall, F. H. Pollak, J. C. Bean, and R. H. Hull, Phys. Rev. B **33**, 6821 (1986).

[5]J. Bevk, J. P. Mannaerts, L. C. Feldman, B. A. Davidson, and A. Ourmazd, Appl. Phys. Lett. **49**, 286 (1986).

[6]F. Cerdeira, A. Pinczuk, J. C. Bean, B. A. Batlogg, and B. A. Wilson, Appl. Phys. Lett. **48**, 1138 (1984).

[7]M. Chandrasekhar and F. H. Pollak, Phys. Rev. B **15**, 2127 (1977).

[8]T. P. Pearsall, J. Bevk, L. C. Feldman, J. M. Bonar, J. P. Mannaerts, and A. Ourmazd, Phys. Rev. Lett. **58**, 729 (1987).

[9]S. Froyen, S. M. Wood, and A. Zunger, Phys. Rev. B **36**, 4574 (1987).

[10]R. People and S. Jackson, Phys. Rev. B **36**, 1310 (1987).

[11]C. Ciraci and I. P. Batra, Phys. Rev. Lett. **58**, 2114 (1987).

[12]M. S. Hybertsen and M. Schlüter, Phys. Rev. B **36**, 9683 (1987).

[13]S. Satpathy, R. M. Martin, and C. G. Van de Walle, Phys. Rev. B **38**, 13 237 (1988).

[14]I. Morrison, M. Jaros, and K. B. Wong, Phys. Rev. B **37**, 9693 (1987).

[15]K. B. Wong, M. Jaros, I. Morrison, and J. P. Hagon, Phys. Rev. Lett. **60**, 2221 (1988).
[16]J. Bevk, B. A. Davidson, L. C. Feldman, H.-J. Gossmann, J. P. Mannaerts, S. Nakahara, and A. Ourmazd, J. Vac. Sci. Technol. B **5**, 1147 (1987).
[17]J. Bevk, A. Ourmazd, L. C. Feldman, T. P. Pearsall, J. M. Bonar, B. A. Davidson, and J. P. Mannaerts, Appl. Phys. Lett. **50**, 760 (1987).
[18]H. Shen, P. Parayanthal, Y. F. Liu, and Fred H. Pollak, Rev. Sci. Instrum. **58**, 1429 (1987).
[19]D. E. Aspnes, in *Handbook on Semiconductors,* edited by M. Balkanski (North-Holland, New York, 1980), Vol. 2, p. 109.
[20]B. V. Shanabrook, O. J. Glembocki, and W. T. Beard, Phys. Rev. B **35**, 2540 (1987).
[21]X. L. Zheng, D. Heiman, B. Lax, and F. A. Chambers, Appl. Phys. Lett. **52**, 287 (1988).
[22]G. D. Sanders and K. K. Bajaj, Phys. Rev. B **35**, 2308 (1987).
[23]Y. R. Lee, A. K. Ramdas, F. A. Chambers, J. M. Meese, and L. R. Ram-Mohan, Appl. Phys. Lett. **50**, 600 (1987).
[24]M.-H. Meynadier, R. E. Nahory, J. M. Worlock, M. L. Tamargo, and J. L. de Miguel, Phys. Rev. Lett. **60**, 1338 (1988).
[25]J. S. Kline, F. H. Pollak, and M. J. Cardona, Helv. Phys. Acta **41**, 968 (1968).
[26]R. People, Phys. Rev. B **32**, 1405 (1985).
[27]C. G. Van de Walle and R. M. Martin, J. Vac. Sci. Technol. B **4**, 1055 (1986).
[28]A. Joullie, A. Z. Eddin, and B. Girault, Phys. Rev. B **23**, 928 (1981).
[29]M. Gnutzmann and K. Clausecker, Appl. Phys. **3**, 9 (1974).
[30]J. A. Moriarity and S. Krishnamurthy, J. Appl. Phys. **54**, 1892 (1983).
[31]W. Ni, J. Knall, and G. V. Hansson, Phys. Rev. B **36**, 7744 (1987).
[32]R. People, J. C. Bean, D. V. Lang, A. M. Sergent, H. L. Störmer, K. W. Wecht, R. T. Lynch, and K. Baldwin, Appl. Phys. Lett. **45**, 1231 (1985).
[33]G. Abstreiter, H. Brugger, T. Wolf, H. Jorke, and H.-J. Herzog, Phys. Rev. Lett. **54**, 2441 (1985).
[34]Sverre Froyen, D. M. Wood, and Álex Zunger, Phys. Rev. B **37**, 6893 (1988).
[35]M. S. Hybertsen, M. Schlüter, R. People, S. A. Jackson, D. V. Lang, T. P. Pearsall, J. M. Vandenberg, and J. Bevk, Phys. Rev. B **37**, 10 195 (1988).
[36]A. Daunois and D. E. Aspnes, Phys. Rev. B **18**, 1824 (1978).
[37]M. Chandrasekhar and F. H. Pollak, Phys. Rev. B **15**, 2127 (1977).
[38]B. O. Seraphin, in *Semiconductors and Semi-metals,* edited by R. Willardson and A. E. Beer (Academic, New York, 1972), Vol. 9, p. 1.
[39]M. Cardona, *Modulation Spectroscopy,* Suppl. 11 of *Solid State Physics,* edited by H. Ehrenreich, F. Seitz, and D. Turnbull (Academic, New York, 1969).
[40]L. Brey and C. Tejedor, Phys. Rev. Lett. **59**, 1022 (1987).
[41]R. Hull, J. C. Bean, F. Cerdeira, A. T. Fiory, and J. M. Gibson, Appl. Phys. Lett. **48**, 56 (1986).
[42]D. Stroud and H. Ehrenreich, Phys. Rev. B **2**, 3197 (1970).
[43]M. S. Hybertsen and M. Schlüter, in *Proceedings of the Materials Research Society Symposium on the Epitaxy of Layered Structures, 1987,* edited by R. T. Tung, L. R. Dawson, and R. L. Gunshor (MRS, Pittsburgh, 1988), Vol. 102, p. 413.

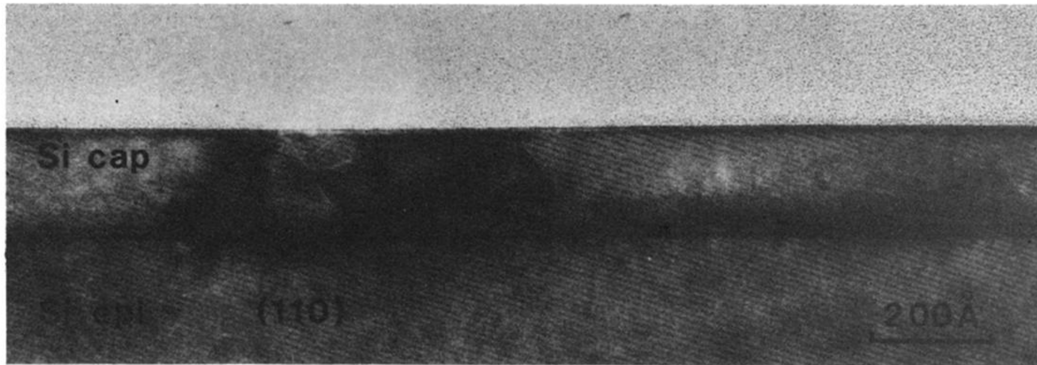

FIG. 10. TEM cross section in the lattice-imaging mode of the (6:6) superlattice structure. The critical thickness limit was exceeded during growth, resulting in an absence of long-range coherent layering of Ge and Si.

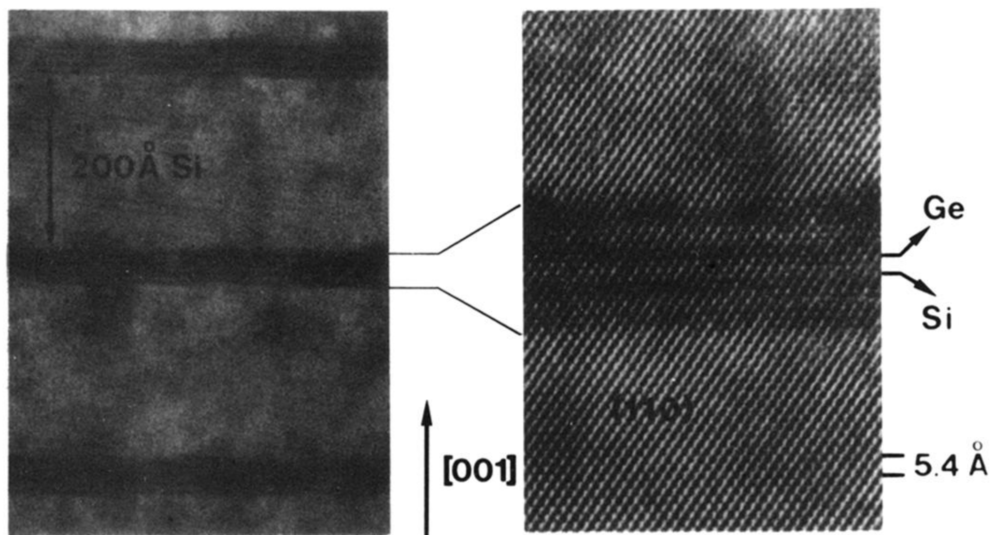

FIG. 7. Transmission micrograph of an extended (4:4) superlattice grown by MBE. Direct lattice imaging is used to resolve pairs of atoms. The lower-magnification cross section of the sample shows that planarity is maintained both laterally and in the growth direction.